Study on Processing of Ultrahigh Molecular Weight Polyethylene/Polypropylene Blends

Gongde Liu, Yingzi Chen, Huilin Li

The State Key Laboratory of Polymer Materials Engineering, Polymer Research Institute of Sichuan University, Chengdu 610065, China

Received 13 November 2003; accepted 24 February 2004
DOI 10.1002/app.20679
Published online in Wiley InterScience (www.interscience.wiley.com).

ABSTRACT: The processing of ultrahigh molecular weight polyethylene (UHMWPE) by the addition of polypropylene (PP) and high-density polyethylene (HDPE) was investigated. The results show that the addition of PP improves the processability of UHMWPE more effectively than does the addition of HDPE. UHMWPE/PP blends can be effectively processed with a twin-roller and general single-screw extruder. In the extrusion of UHMWPE/PP blends, PP is enriched at the surface of the blend adjacent to the barrel wall, thus increasing the frictional force on the wall; the conveyance of the solid down to the channel can then be carried out. The melt pool against the active flight flank exerts a considerable pressure on the UHMWPE powder in the passive flight flank, which overcomes the hard compaction of UHMWPE. The PP penetrates into the gaps between the particles, acting as a heat-transfer agent and adhesive, thus enhancing the heat-transfer ability in the material. © 2004 Wiley Periodicals, Inc. J Appl Polym Sci 94: 977–985, 2004

Key words: polyethylene (PE); polypropylene (PP); processing; extrusion; heat transfer

INTRODUCTION

Ultrahigh molecular weight polyethylene (UHMWPE) is characterized by a number of important properties, including high notched impact strength, energy absorption capacity at high loading rates, resistance to stress cracking, and extremely low embrittlement temperatures. Necessarily at these high molecular weights, the PE displays a high viscosity and pronounced viscoelastic characteristics in the melt that make it unsuitable for conventional processing operations, with the exception of compression molding and ram extrusion.[1,2] Numerous efforts have been made to reduce the viscosity by solution or gel processing.[3–5] Another effective way to reduce the melt viscosity is to dilute the UHMWPE with conventional PE that generally has a lower average molecular weight.[6–8] However, this usually causes a marked decrease in some of the most desirable properties of UHMWPE. Furthermore, to realize effective extruding, the extruder are ameliorated by digging grooves in the extruder barrel to improve the mixing and solid conveying ability of the general single-screw extruder. Application of the grooved barrel extruder often results in extremely high extruding pressure and serious wear on the grooves. In this article, processing of UHMWPE with a twin-roller and general single-screw extruder by the addition of polypropylene is investigated, and a surprisingly improved processability is observed for the UHMWPE/PP blend compared with that for UHMWPE and UHMWPE/high-density polyethylene (HDPE) blend.

Correspondence to: H. Li (lihuilin5405136@sina.com.cn).

Contract grant sponsor: Special Funds for Major State Basic Research Projects of China; contract grant number: G1999064809).

Contract grant sponsor: National Nature Science Foundation of China; contract grant number: 50233010.

Contract grant sponsor: Funds for Doctoral Disciplines of Ministry of Education of China.

EXPERIMENTAL

Materials

UHMWPE (M-II), with an average molecular weight of 2.5×10^6 and a mean particle diameter of about 300 μm, was supplied by Beijing No. 2 Auxiliary Agent Factory (Beijing, China). PP (F401) was supplied by Lanzhou Chemical Industry Factory (Lanzhou, China) with a melt flow rate (MFR) of 2.0 g/10 min (230°C, 2.16 kg load). HDPE (5000S) was supplied by Yanshan Petrochemical Corp. (Beijing, China) with MFR = 1.2 g/10 min (230°C, 2.16 kg load). HDPE (6098A) was supplied by Qilu Petrochemical Corp. (Shangdong, China) with MFR = 7.8 g/10 min (230°C, 2.16 kg load).

Processing experiments and evaluation

The plasticating experiments of UHMWPE/polypropylene (PP) blends were carried out with a twin-roller

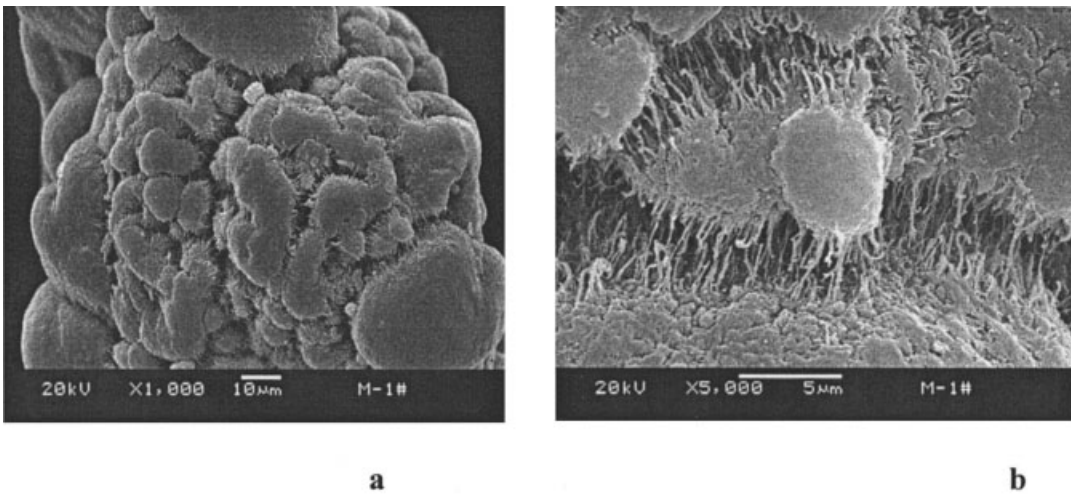

Figure 1 SEM micrographs of the as-received UHMWPE powder at magnifications of (a) ×1000 and (b) ×5000.

at 200°C. The extrusion experiments were carried out with a general three-section single-screw extruder (D = 25 mm, L/D = 25) through a circle die. The temperatures for every section of the barrel were 100, 190, and 230°C, respectively, and 210°C for the die.

The specimens for FTIR and thermal analysis were sliced carefully from the sample at different axial locations along the screw. FTIR analysis was carried out with a Nicolet-560 FTIR instrument (Nicolet Analytical Instruments, Madison, WI). The thermal characteristics were studied on Netzsch DSC 204 (Netzsch-Gerätebau GmbH, Bavaria, Germany). The samples were heated under nitrogen atmosphere from 40 to 200°C at a rate of 10°C/min.

A JSM 5900 LV scanning electron microscope (SEM; JEOL, Tokyo, Japan) was used to observe microphotographs of the morphology of the specimens.

An atomic force micrograph (AFM, SPA400, Seiko Instruments Inc., Chiba, Japan), measuring in the tapping mode, was applied to investigate the morphology of the skin and center specimens. Before the AFM observation, the specimens were etched in a solution of 1.3 wt % $KMnO_4$ dissolved in a $H_2SO_4/H_3PO_4/H_2O$ (10 : 4 : 1) mixture to eliminate the amorphous phase.

X-ray diffraction measurements were taken on a Philips X'pert pad diffractometer (Philips, Eindhoven, The Netherlands) with Cu–K_α radiation. The accelerating voltage and electric current used were 10 kV and 40 mA, respectively. The scan range was 10–40° (2θ, Bragg's angle), and the glancing angles were 0.25, 7, and 15°.

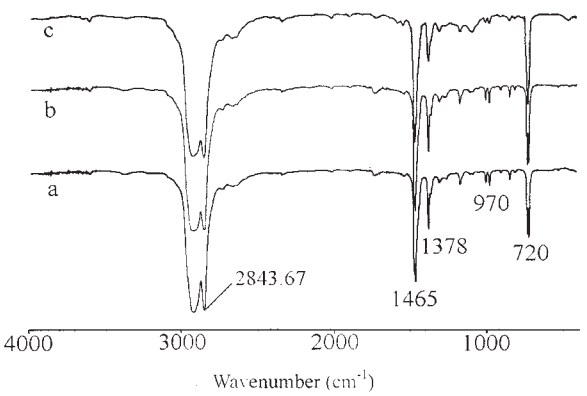

Figure 2 FTIR spectra of skin layer of UHMWPE/PP (80 : 20) plasticating time: (a) 4 min; (b) 7 min; (c) 10 min.

RESULTS AND DISCUSSION

Nascent UHMWPE M-II powder

Figure 1(a) and (b) show SEM micrographs of the as-received M-II powder at two magnifications. The powder is made up of major particles with an average diameter of about 300 μm, and these major particles are in turn made up of minor particles with diameters of about 10 μm. The minor particles are aggregates of yet smaller, submicron particles. Some fibrillar bridges between these discrete particles indicate partial melting during synthesis.

Plasticating of UHMWPE/PP blend with a twin roller

UHMWPE/PP (80 : 20 by weight) blends were plasticated at 200°C with a twin roller for different times,

TABLE I
Relative Absorbance Intensity of PP and UHMWPE in the Specimens

	Plasticizing time (min)		
	4	7	10
A_{970}/A_{720}	0.218	0.191	0.084

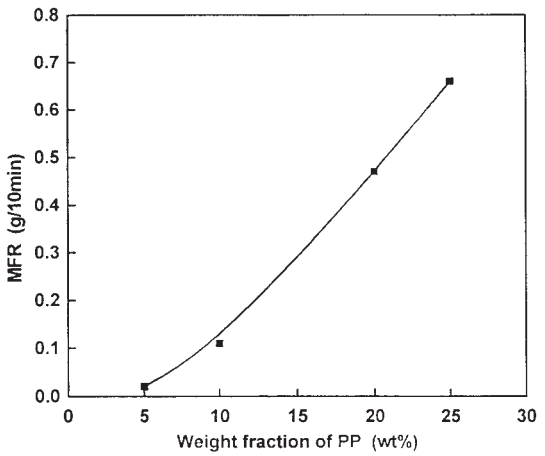

Figure 3 Melt flow rate of UHMWPE/PP blends versus weight fraction of PP.

and the skin specimens were carefully sliced off from the plasticated sheet. Figure 2 shows the FTIR spectra of the skin specimens with plasticating times of 4, 7, and 10 min, respectively. The absorbance bands around 970 cm^{-1} are associated with $[CH_2CH(CH_3)]_n$ of PP, and the bands around 720 cm^{-1} are associated with $[CH_2]_n$ ($n \geq 4$) of UHMWPE. The ratios of the absorbance bands area of PP (A_{970}) to that of UHMWPE (A_{720}) are used to denote the relative strength of the characteristic absorbance bands of PP and UHMWPE, as shown in Table I. The ratio falls off with increasing plasticating time, which indicates that the PP content in the skin specimens decreased with increasing plasticating time.

SEM observation of the original UHMWPE powder revealed that the major UHMWPE particles consist of minor particles. The low mobility of the molecular chain and the gaps that exist between the particles retard the transmission of heat within the material

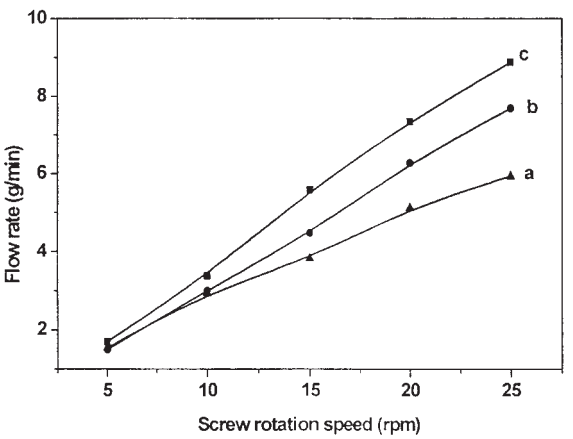

Figure 4 Variation of flow rate of UHMWPE/PP blends, with screw rotation speed, at various proportions: (a) 90 : 10; (b) 80 : 20; (c) 70 : 30.

TABLE II
Die Pressure of UHMWPE/PP and UHMWPE/PE Blends Extrudated with Single-Screw Extruder[a]

Sample	Content (wt %)	Die pressure (MPa)
PP	10	3.9–4.3
	20	3.1–3.4
	30	2.8–3.1
HDPE (5000S)	20	0–8.2
HDPE (6098A)	20	0–6.8
HDPE (6098A)	30	0–5.6

[a] Screw rotation speed: 10 rpm.

during processing. UHMWPE is thus not processable through use of the general processing technique. In the case of UHMWPE/PP blend, the molten PP does not tend to penetrate into the UHMWPE domains because of the poor miscibility of UHMWPE and PP. The molten PP prefers to flow into the gaps between particles and the skin layer, which increases the stickiness of the melt to the roller surface and the adhesive banding between particles. Therefore, UHMWPE/PP blends are plastic with a twin roller. With increasing plasticating time, greater amounts of PP penetrate into the gaps, and the PP content in the skin decreases.

However, the plasticating of UHMWPE/HDPE by a twin roller is exceedingly difficult under the same condition. It was confirmed that the UHMWPE/HDPE (80 : 20) blend is plastic during the first few minutes, and the melt sheet could be peeled off from the roller. With increasing plasticating time, the melt sheet fragments. Because of the good miscibility of UHMWPE and HDPE, the molten HDPE rapidly penetrated into the UHMWPE domains within the first few minutes during processing. With increasing plasticating time, an insufficient HDPE melt exists in the skin of the specimens and the gaps between the particles, thus hindering the plasticating of UHMWPE/HDPE blends.

Figure 3 shows that the addition of PP does improve

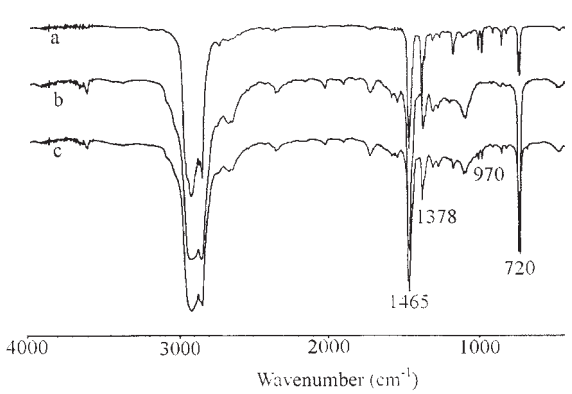

Figure 5 FTIR spectra of the sliced specimens (1st section): (a) outer skin; (b) center; (c) inner skin.

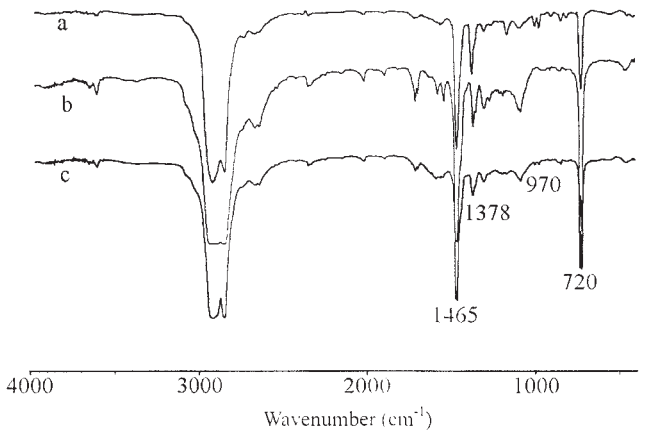

Figure 6 FTIR spectra of the sliced specimens (2nd section): (a) outer skin; (b) center; (c) inner skin.

the fluidity of UHMWPE: the MFR of the UHMWPE/PP blends increases steadily with increasing PP content in the blends.

Extrusion experiments with a single-screw extruder

Figure 4 shows that the flow rate of UHMWPE/PP blends increases steadily with increasing screw rotation speed. The greater the amount of PP contained in the blend, the faster the flow rate increased. No blockade occurred at a high extrusion speed, which often occurs in the extrusion of UHMWPE/HDPE blends with a general single-screw extruder.

Because of their similar structure and good compatibility, various polyethylenes (HDPE, LDPE, MMPE, etc.) are usually used as processing aid agents of UHMWPE. Table II shows the effect of PP and HDPE on the processability of UHMWPE. When the PP content is 10 wt % in the UHMWPE/PP blend, the die pressure is very stable during extrusion, and it decreases accordingly with increasing PP content. However, the extrusion of UHMWPE/HDPE blends with a general single-screw extruder is very difficult. The die pressure is much higher than that of the UHMWPE/PP blend, and a blockade occurred from time to time. It is very interesting to note that, when the blockade occurred during the extrusion of UHWMEP/HDPE blends, the addition of some PP into the barrel effectively solves the problem, whereas

TABLE III
Relative Absorbance Intensity of PP and UHMWPE in the Specimens

	A_{970}/A_{720}		
Section	Outer skin	Center	Inner skin
1st	0.502	0.025	0.089
2nd	0.187	0.027	0.031

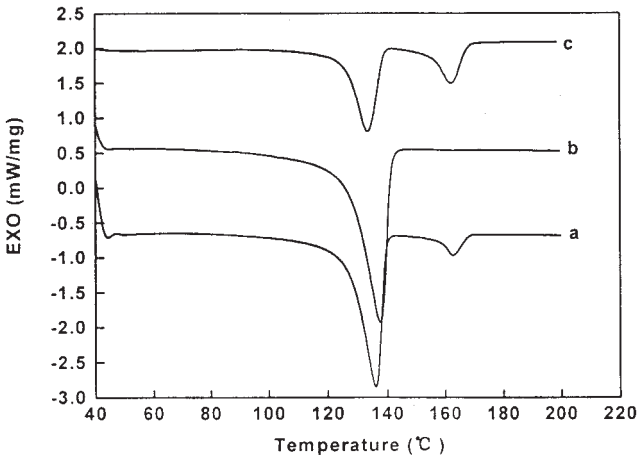

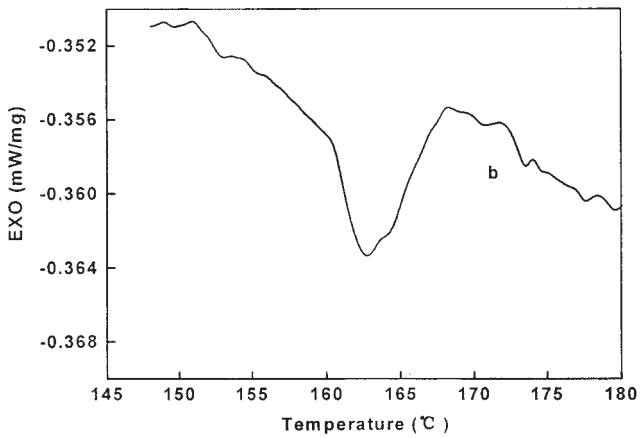

Figure 7 DSC curves of the sliced specimens (1st section): (a) inner skin; (b) center; (c) outer skin.

the addition of HDPE does not. This indicates that PP is much more efficient than HDPE in aiding the extrusion of UHMWPE.

The mechanical properties of UHMWPE/PP blends, reported in a previous study,[10] indicated that when PP is added, the Young's modulus, yield strength, and Izod notched impact strength are increased at optimized PP content.

Extrusion mechanism of UHMWPE/PP blends with a general single-screw extruder

Solid conveying, plasticating (or melting), and melt conveying (or pumping) are the main functions of a single-screw extruder. The first comprehensive analysis of solids transport in a single-screw extruder was reported nearly five decades ago by Darnell and Mol.[9] The general approach to solids conveying analysis is to consider an element of the solid bed in the screw channel and determine all forces that are acting on the element. The frictional forces at the boundaries and the forces resulting from pressure gradients in the

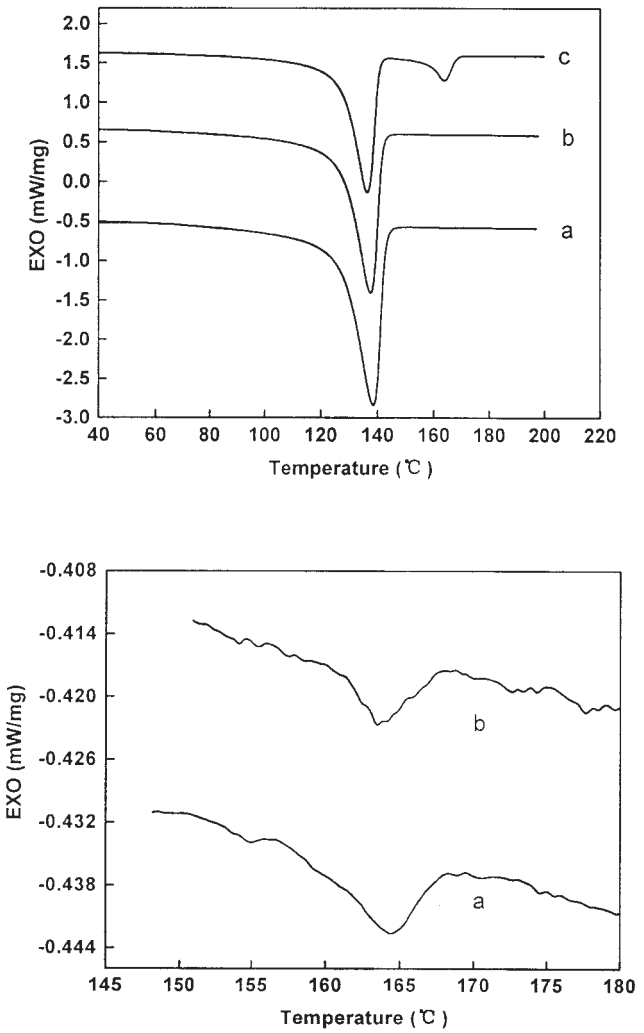

Figure 8 DSC curves of the sliced specimens (2nd section): (a) inner skin; (b) center; (c) outer skin.

solid bed are the most important forces to consider. For optimum solids conveying, the frictional force on the barrel should be maximum and the frictional force on the screw should be minimum. If the frictional force on the barrel is zero, no forward transport will occur. If the frictional force on the screw is zero, maximum forward transport will occur.

The low coefficient of friction, absence of stickiness to the barrel wall, and extremely high melt viscosity of UHMWPE make it impossible to extrude with a general single-screw extruder. Actually, a surprisingly improved processability is observed for the UHMWPE/PP blend compared with that for UHMWPE and the UHMWPE/HDPE blend. PP must play a prominent role in the extrusion of the UHMWPE in the extruder.

To study the mechanism for the extrusion of UHMWPE with the addition of PP, the experiments were based on screw-extraction experiments, in which the screw is stopped during the extrusion and drawn out of the barrel with the material still adhering to it. The material in the screw channel is analyzed at various axial locations along the screw.

FTIR analysis of the specimens

Figures 5 and 6 show the FTIR spectra of the specimens obtained from the feeding section (1st section) and the compression section (2nd section) of the screw, respectively. For each section, three specimens were taken at different locations along the screw radial direction: (1) the surface adjacent to the barrel (outer skin), (2) the center, and (3) the surface adjacent to the screw (inner skin). The ratios of the adsorbance band area of PP (A_{970}) to that of UHMWPE (A_{720}) are listed in Table III, which indicates that for the 1st section, the PP content is greatest in the outer-skin specimens and least in the core specimens, and the PP content of the inner-skin specimens is much lower than that in the outer-skin specimens. The specimens taken from the 2nd section demonstrate a similar PP distribution. Increased amounts of PP on the barrel wall increase the stickiness and friction force of UHMWPE to the barrel wall, and thus the processability of UHMWPE is substantially improved.

The specimens sliced off from the different sections were analyzed by DSC to further verify the PP distribution in the barrel (Figs. 7 and 8). Table IV summarizes the values obtained from DSC thermograms.

The melting peak, appearing in the DSC thermograms at 136°C, corresponds to the melting of crystallized UHMWPE, and the peak at 164°C is attributed to the melting of crystallized PP in the UHMWPE/PP blend. The relative contents of PP in the specimens are denoted by the ratio of PP crystal melting enthalpy to that of UHMWPE (Table IV), which indicates that the outer-skin specimens contain the most PP, and the center specimens contain the least PP, which is consistent with the results of FTIR analysis, mentioned earlier.

The morphology of the specimens taken from the 1st section was studied by AFM in the tapping mode. Figure 9(a) shows the AFM micrograph of pure PP, which shows a typical spherical crystal structure. Figure 9(b) shows the characteristic crystal structure of

TABLE IV
DSC Data of the Specimens

Section	Specimen	ΔH_{UHMWPE} (J/g)	ΔH_{PP} (J/g)	$\Delta H_{PP}/\Delta H_{UHMWPE}$ (%)
1st	Outer skin	68.03	32.16	47.29
	Inner skin	125.5	13.27	10.57
	Center	167.2	0.27	0.16
2nd	Outer skin	112.2	15.06	13.42
	Inner skin	151.8	0.21	0.14
	Center	186.0	0.15	0.08

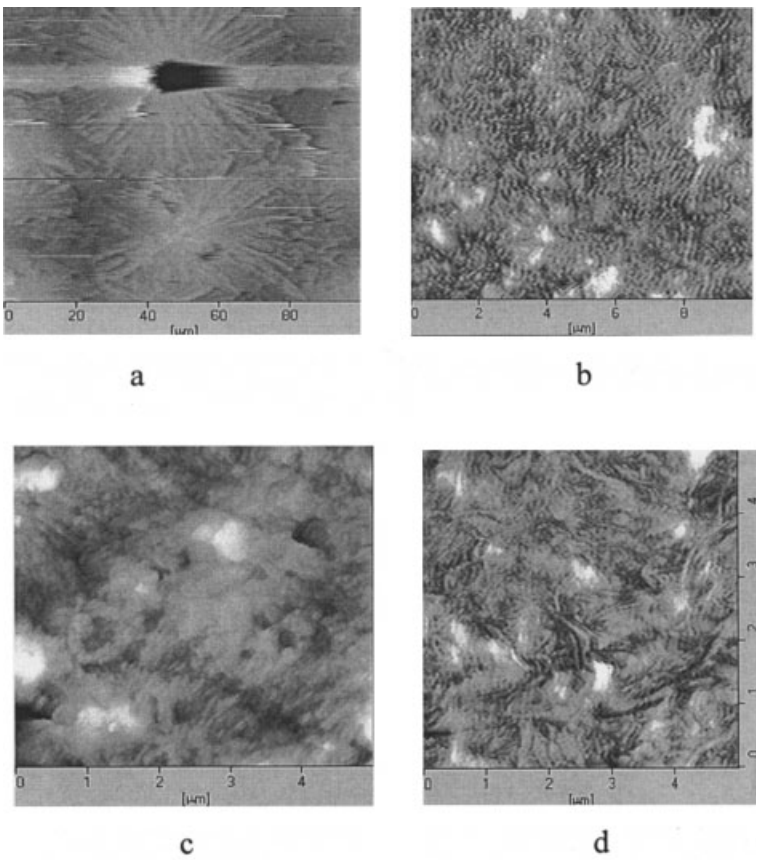

Figure 9 AFM micrographs of the specimens: (a) PP; (b) UHMWPE; (c) UHMWPE/PP (80 : 20), outer skin; (d) UHMWPE/PP (80 : 20), center.

pure UHMWPE. The AFM micrograph of the outer-skin specimen of the UHMWPE/PP (80 : 20) blend displays a crystal morphology similar to that of PP, as shown in Figure 9(c); and the core specimen displays a crystal morphology similar to that of UHMWPE, as shown in Figure 9(d). Therefore, it is concluded that the outer-skin specimen primarily consists of PP and the core specimen consists mainly of UHMWPE, which is consistent with the results obtained above.

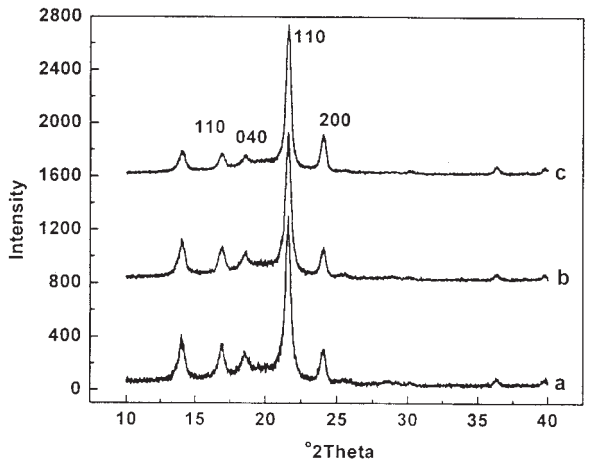

Figure 10 WAXD diffractograms of the specimen at different glancing angles: (a) 0.25°; (b) 7°; (c) 15°.

Figure 10 shows the X-ray diffraction patterns of the UHMWPE/PP (80 : 20) blend at different glancing angles. The specimens are taken from the 1st section. The peaks at 16.8 and 18.4° are the reflections of [110] and [040] planes of α-PP; the peaks at 21.5 and 23.9° correspond to the [110] plane and [200] plane of UHMWPE, respectively. The intensity of [110] and [040] diffraction peaks of α-PP decreases with increasing glancing angle.

$$l_{\max} = \frac{3.2}{\mu_l} \sin\theta \tag{1}$$

TABLE V
Relative Intensity of [110] and [040] of α-PP with the Glancing Angle

Glancing angle, θ (°)	Depth ($1/\mu_l$)	[*hlk*]	Relative intensity (%)	[*hlk*]	Relative intensity (%)
0.25	0.0141	110	24.87	040	19.43
7	0.3901	110	23.47	040	16.5
15	0.8282	110	13.55	040	9.41

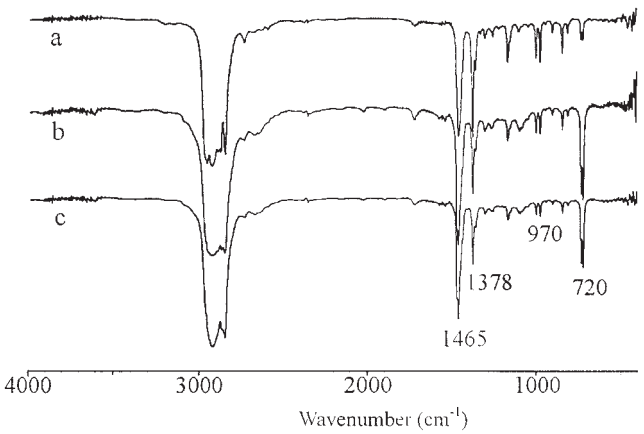

Figure 11 FTIR spectra of the specimens in active flight flank: (a) 1st section; (b) 2nd section; (c) 3rd section.

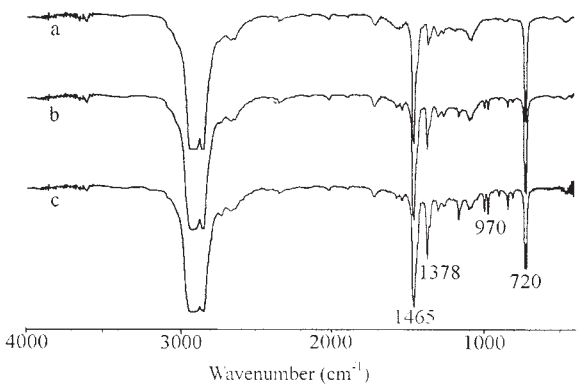

Figure 12 FTIR spectra of the specimens in passive flight flank: (a) 1st section; (b) 2nd section; (c) 3rd section.

where l_{max} is the largest depth tested, θ is the glancing angle, and μ_l is the linear adsorption coefficient.

According to the formula, the greater the glancing angle, the deeper the specimen will be tested. The relative intensities of [110] and [040] diffraction peaks of α-PP to that of the [110] plane of UHMWPE are listed in Table V. The relative intensities of [110] and [040] diffraction peaks of α-PP decrease with increasing glancing angle, which indicates that the PP content in the specimen decreases with the specimen depth increasing from the outer surface toward the center.

TABLE VI
Relative Absorbance Intensity of PP and UHMWPE in the Specimens

	A_{970}/A_{720}		
Flight flank	1st section	2nd section	3rd section
Active	1.750	0.229	0.205
Passive	0.008	0.072	0.239

With increasing amounts of PP on the barrel wall, the friction force on the wall and the stickiness of the melt to the barrel are increased, such that the extrusion of the UHMWPE/PP blend with a general single-screw extruder is achieved.

Plasticating of UHMWPE/PP blends in the barrel during extrusion

The second functional zone in the extruder is the plasticating zone or melting zone. For the UHMWPE/PP blend, although the crystal melting temperature of UHMWPE is lower than that of PP, the molten UHMWPE does not flow and does not stick to the barrel; therefore the melt film aggregated on the barrel wall should be PP. Because of the immiscibility of UHMWPE and PP, the molten PP cannot penetrate into the UHMWPE domains. As the screw proceeds, the PP melt flow from the barrel wall to the active flank forms a melt pool, which exerts high pressure on the UHMWPE powder against the passive flight flank, thus compressing it to a compacted solid bed.

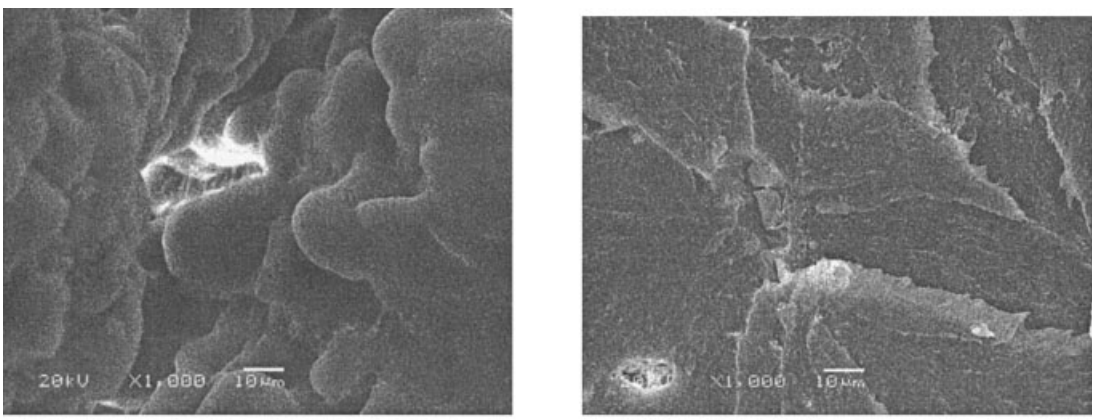

Figure 13 SEM micrographs of the specimens: (a) 1st section; (b) 3rd section.

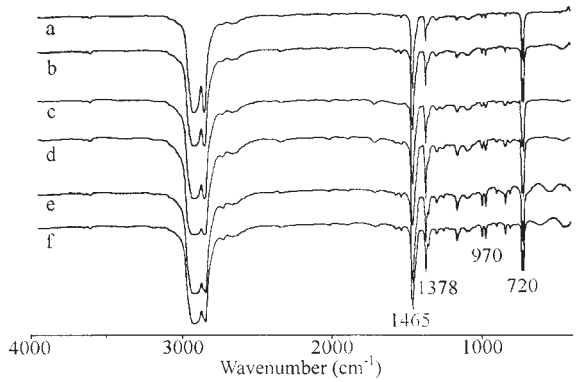

Figure 14 FTIR spectra of the UHMWPE/PP extrudate. UHMWPE/PP (90 : 10): (a) skin; (b) core; UHMWPE/PP (80 : 20): (c) skin; (d) core; UHMWPE/PP (70 : 30): (e) skin; (f) core.

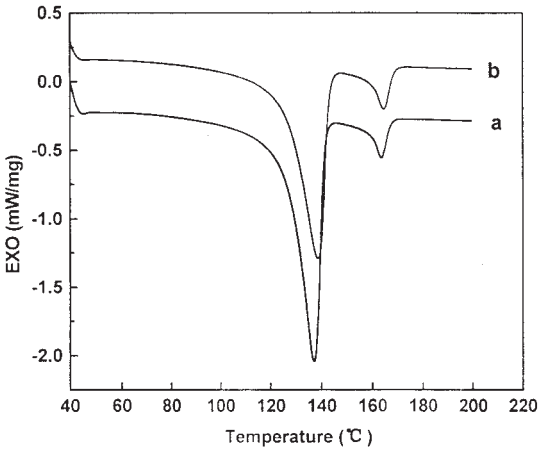

Figure 15 DSC curves of UHMWPE/PP (80 : 20) extrudate: (a) skin; (b) core.

Figure 11 shows the FTIR spectrum of specimens against the active flight flank from the 1st section to the 3rd section. As the material proceeds in the barrel, the PP content against the active flank decreased. On the contrary, the PP content against the passive flight flank increased from the 1st section to the 3rd section, as shown in Figure 12. The specimens against the active and the passive flight flanks of the 3rd section demonstrate similar characteristic absorbance bands of PP in the FTIR spectra [Fig. 11(c), Fig. 12(c), and Table VI], which indicates that in the 3rd section of the extruder, the mixing and plasticating of UHMWPE and PP have almost been completed.

Figure 13 shows the SEM micrographs of specimens against the passive flight flank of the 1st and the 3rd sections. The specimen from the 1st section has a morphology similar to that of the original UHMWPE powder. Some fibrillar structure appears between the particles, attributed to the heat fusion, whereas the specimens from the 3rd section demonstrate a dense morphology structure, which indicates that the component in the blend had been completely plasticated in the 3rd section.

Figure 14 shows the FTIR spectra for the skin and core specimens of the extrudate of UHMWPE/PP blends with different PP contents. The ratios of the characteristic absorbance bands area of PP to that of UHMWPE (A_{970}/A_{720}) are listed in Table VII. The relative intensity of PP absorbance bands increases with increasing PP content. The core specimens show more intense PP absorbance than the skin specimens do, as shown in Table VII, which indicates that the PP content in the skin of the extrudate is lower than that in the core.

For the high degree chain entanglement of UHMWPE, the mixing of UHMWPE with PP is rather difficult. After the intense shearing and squeezing through the pumping section, the mixing of the two materials will be more homogeneous, and a greater amount of PP penetrated into the gaps between the UHMWPE major and minor particles, to act as a heat-transfer agent and adhesive between particles. Therefore, the PP content in the skin is less than that in the core of the extrudate. With the increase of PP add-on, the PP located in the gaps becomes saturated, such that the difference of PP content in the skin and core specimens decreases.

The DSC curves of the core and skin specimens of the extrudate are shown in Figure 15. The enthalpy of PP crystal in the core specimen is higher than that in the skin specimens, and the enthalpy of UHMWPE in the core specimens is less than that in the skin specimens, as shown in Table VIII. This reveals that the skin specimens contain less PP, and the core specimens contain more PP.

FTIR analysis of the specimens at different plasticating times by twin roller also revealed that the PP content in the skin specimen decreases with increasing

TABLE VII
Relative Absorbance Intensity of PP and UHMWPE in the Specimens

	A_{970}/A_{720} of UHMWPE/PP		
	(90 : 10)	(80 : 20)	(70 : 30)
Skin	0.072	0.128	0.260
Core	0.142	0.200	0.323

TABLE VIII
DSC Data of the Core and Skin Specimens

UHMWPE/PP (80 : 20)	UHMWPE		PP	
	T_{peak} (°C)	ΔH (J/g)	T_{peak} (°C)	ΔH (J/g)
Skin	137.19	123.9	163.59	11.76
Core	138.69	108	164.49	13.15

plasticating time, which is consistent with the phenomenon discussed above.

CONCLUSIONS

1. The processability of UHMWPE is improved more effectively by the addition of polypropylene (PP) than by HDPE. UHMWPE/PP blends can be effectively processed with a twin-roller and a general single-screw extruder.
2. During the extrusion of UHMWPE/PP blends, PP is enriched at the surface of the blend adjacent to the barrel wall. This increases the frictional force on the wall, so that conveyance of the solid down to the channel could be carried out. The PP penetrates into the gaps between the particles, acting as a heat-transfer agent and adhesive, which enhance the heat-transfer ability in the material.
3. The melt pool against the active flight flank exerts considerable pressure on the UHMWPE powder in the passive flight flanks, and thus the problem of hard-compacted UHMWPE is overcome.
4. The PP content in the skin specimens of the extrudate is lower than that in the core specimens. With increasing PP additions in the blend, the difference in PP content between the skin and the core specimens decreases.

This work was supported by Special Funds for Major State Basic Research Projects of China (Grant G1999064809), National Nature Science Foundation of China (Grant 50233010), and Funds for Doctoral Disciplines of Ministry of Education of China.

References

1. Zacbarriades, A. E.; Kanamoto, T. AIChE Annu Meet Symp 1984, 25.
2. Whitehouse, C.; Liu, M. L.; Gao, P. Polym Eng Sci 1999, 39, 904.
3. Smith, P.; Lemstra, P. J. J Mater Sci 1980, 15, 505.
4. Mastuo, M.; Manley, R. Macromolecules 1982, 15, 985.
5. Anton, C.; Mackiey, M. R.; Solbal, S. B. Polym Bull 1987, 17, 175.
6. Parimal, V.; Thein, K. Polym Eng Sci 1987, 27, 202.
7. Scheetz, H. A.; Gilles, R. C. U.S. Pat. 4,281,070, 1981.
8. Bin, Y.; Lin, M.; Alachi, R. Polymer 2001, 42, 8125.
9. Darnell, W. H.; Mol, A. J. Soc Pet Eng J 1956, 12, 20.
10. Liu, G.; Li, H. J Appl Polym Sci 2003, 89, 2628.